Journal of
Food Chemistry & Nanotechnology

https://doi.org/10.17756/jfcn.2023-154

Research Article

Open Access

# Anti-moulding Activity of Oleylamine-capped Silver Nanoparticles

**John Kimagut Mining[1], Makwena Justice Moloto[2*], Wesley Nyaigoti Omwoyo[3], Dominic Menge[4] and Winny Kgabo Maboya[1]**

*[1]Department of Biotechnology and Chemistry, Faculty of Applied and Computer Sciences, Vaal University of Technology, Private Bag X021, Vanderbijlpark, South Africa*
*[2]Institute for Nanotechnology and Water Sustainability, College of Science, Engineering, and Technology, 28 Pioneer Avenue, Florida Campus, University of South Africa, South Africa*
*[3]Department of Mathematics and Physical Sciences, School of Pure, Applied and Health Science (SPAHS), Maasai Mara University, Narok, Kenya*
*[4]Department of Biological Sciences, School of Pure, Applied and Health Sciences (SPAHS), Maasai Mara University, Narok County, Kenya*

***Correspondence to:**
Makwena Justice Moloto
Institute for Nanotechnology and Water Sustainability, College of Science, Engineering, and Technology, 28 Pioneer Avenue, Florida Campus, University of South Africa, South Africa.
**E-mail:** molotmj@unisa.ac.za

**Received:** June 28, 2023
**Accepted:** July 21, 2023
**Published:** July 26, 2023

**Citation:** Mining JK, Moloto MJ, Omwoyo WN, Menge D, Maboya WK. 2023. Anti-moulding Activity of Oleylamine-capped Silver Nanoparticles. *J Food Chem Nanotechnol* 9(2): 88-93.

**Copyright:** © 2023 Mining et al. This is an Open Access article distributed under the terms of the Creative Commons Attribution 4.0 International License (CC-BY) (http://creativecommons.org/licenses/by/4.0/) which permits commercial use, including reproduction, adaptation, and distribution of the article provided the original author and source are credited.

Published by United Scientific Group

## Abstract

Moulds are filamentous fungus that may grow on a wide range of surfaces, including built surfaces, food, decaying organic debris, and humid environments. Mould development is distinguished by an unpleasant odour and an unsightly look in confined or non-ventilated areas. They pose a health risk due to their propensity to create and release mycotoxins, which are harmful to both animals and humans. This research aimed to assess the antifungal activity of silver nanoparticles (AgNPs) capped with oleylamine (OLA), which can be utilized to effectively inhibit mould development. The produced AgNPs had a maximum absorbance at 409 nm in the ultraviolet-visible (UV-Vis) spectrum and a particle size of 8.44 ± 1.73 nm, from transmission electron microscopy (TEM) images. The OLA-capped AgNPs had a face-centred cubic (fcc) structure, comparable to bulk silver, with diffraction peaks at 38.3°, 44.5°, 64.7° and 77.9°, which are indexed to the (111), (200), (220) and (311) lattice planes. The existence of elemental silver was confirmed using energy dispersive spectroscopy (EDS) which showed the predominant amount of silver, oxygen, and carbon. Tests for fungal growth that causes mould revealed that AgNPs remarkably inhibit growth in a dose-dependent manner.

## Keywords

Silver, Mould, Nanoparticles, Oleylamine, Antibacterial, Antifungal

## Introduction

Food commodities are crucial in developing nations, where bulk cereal grains used for food and feed are the principal exports. Cereal grains may get contaminated with a filamentous fungus that creates mycotoxins due to unfavourable pre-crop, storage, and post-harvest environments [1-3]. Mycotoxins are secondary metabolites that fungi make as part of their regular metabolic activities [4]. They are not required for the existence of the organism that produces them but frequently aid in defense, communication, or other specialized tasks. Mycotoxins are created by fungi to compete with other species for resources such as nutrition or living space [5]. Mycotoxins are classified into several classes, including aflatoxins, ochratoxins, trichothecenes, and fumonisins. Each of these kinds of mycotoxin has a unique chemical structure, method of action, and toxicity profile [6]. The most prominent mycotoxins are mainly produced by toxigenic species of *Aspergillus* [7].

Moulds pose a substantial risk to agricultural and post-harvest grain crops by increasing the likelihood of damage. They have an impact on both the quality

and quantity of the grains. Moulds may develop on a variety of surfaces, including buildings (both inside and outdoors), food, decomposing organic debris, and any moist environment [8, 9]. Their development is distinguished by an awful odour and an aesthetic appearance [10]. Furthermore, they pose a public health risk since particular strains discharge chemicals and spores into the environment, causing allergic sensitivity and other illnesses like cancer [3, 11]. Their growth has an impact on grain quality, posing a danger to the economy and food security. They inflict severe harm to the grain, reducing the nutritional content and germination ability of the seeds. Mould development continues to be a significant issue for farmers during grain storage. They promote grain heating and hot spot development, as well as grain crusting, dry matter loss, nutritional value reduction, and seed germination losses [12-14]. The development of novel antifungal agents has always been in high demand due to the increase of resistant fungal isolates and the necessity to manufacture antifungals with lower toxicity and lower cost [15]. Antifungal resistance has arisen globally as a result of the frequent use of agrochemicals and/or a shift in the fungal population, favouring the selection of resistant variants [16]. Various technological and innovative solutions for fungal manifestations have been used including nanotechnology [17-19].

Nanotechnology enables the development of novel antifungal chemicals to reduce the impact of developing resistant fungi [20]. NPs, such as AgNPs, have long been utilized as antibacterial agents and are particularly efficient against fungal pathogens [21]. Many mechanisms of action exist for AgNPs, including linkage to phosphate groups in DNA, interaction with the plasma membrane leading to proton dissipation and cell death [22], reaction with sulfhydryl groups of proteins and enzymes, interfering with the electron transport chain, and disrupting membrane permeability to protons and phosphate groups [23]. Silver is a highly appealing metal due to its outstanding size and shape-dependent optical characteristics, the best plasmon excitation efficiency, and the highest electrical and thermal conductivity in bulk among all metals [24-26]. AgNPs' distinct features have led to potential applications in catalysis for the selective oxidation of styrene, ecologically friendly antimicrobial coatings, real-time optical sensors, printed electronics, and photonics [21, 23]. Due to their antifungal effect, AgNPs have the potential to inhibit the growth of moulds [27]. AgNPs are environmentally safe and less toxic for human beings [28]. AgNPs of various sizes and shapes have been shown to exhibit excellent antibacterial activity when compared to other metal NPs [29]. This study focused on the synthesis of AgNPs capped with OLA and investigate their activity against selected species of fungi for their potential anti-moulding application on cereals (beans) during storage. The AgNPs with a potential to embedded into the storage bags for agricultural purpose can provide a good alternative towards use of fungicides. The organic moiety of the capping agent can be removed using hydrophibic-hydrophilic exchange to provide lesser or no interaction with the agricultural products.

# Materials and Methods

## Chemical reagents and materials

Silver nitrate ($AgNO_3$, AR, Merck), toluene (AR, Fisher), oleylamine (70%), ethanol (99%) were obtained from Merck, South Africa. All other solvents and reagents used in this research were of analytical grade. *Candida albicans* ATCC14053, *Cryptococcus neoformaus* ATCC14116, *Aspergillus flavus* ATC9643, and *Aspergillus niger* ATCC168 strains were used for antifungal activity. Deionized water was used throughout the experiment.

## Experimental procedures

### Synthesis of OLA-capped AgNPs

The AgNPs were synthesized using OLA as a capping agent. $AgNO_3$ (0.5 g) was weighed and transferred into a three-neck round bottom flask, followed by the addition of 6 ml of OLA and heated to 180 °C with stirring for one hour. The solution was allowed to cool to 70 °C, centrifuged at 10,000 rpm and then washed three times in ethanol. The supernatant was discarded, and particles were dried in the fume hood, and then packaged for characterization and anti-moulding tests.

### Characterization

The UV-Vis absorption spectra of the OLA-capped AgNPs were recorded at room temperature using a glass cuvette with a 1 cm optical path on a UV-3150 spectrophotometer (Shimadzu, Japan). Fourier Transform Infrared (FTIR) spectra were recorded and captured using a Nicolet Is50 FT-IR with a resolution of 4 $cm^{-1}$ in the wavenumber range 400 - 4000 $cm^{-1}$. The size and structure of produced OLA-capped AgNPs were characterized using TEM. For 15 minutes, the sample was sonicated (Vibronics VS 80). The solution was then dropped onto carbon-coated copper grids. For 30 minutes, the solvent was allowed to evaporate under Infrared light. TEM tests were carried out using a Philips model CM 200 equipment with a 200 kV accelerating voltage. The existence of distinct elemental compositions in the sample was investigated utilizing the Tescan MIRA high-resolution Field Emission-Scanning Electron Microscope coupled with thermo-EDS. The synthesized AgNPs were isolated by centrifugation for 30 minutes at 4000 rpm. The pellets were collected and dried in a 50 °C oven to eliminate excess water before being cooled to room temperature and analyzed for elemental content. The Shimadzu-X-ray Diffraction (XRD) 700 X-ray diffractometer with Cu Ka radiation (λ-1.154056 Å) was used to analyze the XRD patterns. The scan speed was 1°/minute, the current was 30 mA, and the voltage was 40 kV. Following the fitting XRD slot, the samples were placed in a sample holder.

### Antifungal activity of synthesized AgNPs

Agar well diffusion experiment was used for testing the antifungal activity of OLA-capped AgNPs against four fungal strains. Freshly cultivated fungal suspensions (100 L) were aseptically swabbed on Muller-Hinton agar plates, and wells were formed using a sterile cork borer. The OLA-capped AgNPs were put into the wells at varying concentrations (15, 30, 45, and 60 g/ml). The plates were incubated for 24 hours at 37 °C, and the zone of inhibition (ZOI; mm) that formed around the wells was measured.

# Results and Discussion

## Spectroscopic analysis

Figure 1 depicts the UV-Vis absorption spectra of OLA-capped AgNPs. Only a single, narrow, symmetric extinction peak of about 409 nm was observed in the absorption spectra, which is mostly ascribed to primary dipolar excitation. The appearance of a single excitation peak indicated that the OLA-capped AgNPs synthesized were pure. According to published research, the typical absorption peak for AgNPs emerges from 390 to 420 nm. The size of the AgNPs increases with the proximity of the peak to 420 nm [30-32].

To establish the existence of functional groups and their potential interactions with each other and NPs, FTIR spectral analysis was carried out (Figure 2). The FTIR spectrum of OLA-capped AgNPs revealed the absorption peaks at wavenumbers 3303, 3003, 2919, 2856, 2158, and 1648 $cm^{-1}$ comparable to the uncoordinated OLA peaks (3296, 3006, 2922, 2854, 1656 $cm^{-1}$ with two additional peaks at 1608 and 1464 $cm^{-1}$). The amine group (-$NH_2$) showed distinctive peaks in the spectrum of AgNPs at 3303 $cm^{-1}$ and 1648 $cm^{-1}$. The symmetric and asymmetric vibrations of the -$CH_2$ group peaked at 2954 and 2922 $cm^{-1}$, respectively. These peaks maxima are blue-shifted by 2 $cm^{-1}$ in the spectra of OLA-capped AgNPs, which may be due to the capping molecular movements being constrained as a result of the creation of a relatively dense OLA layer on the AgNPs surface [33]. These very minor changes have also been seen in AgNPs with dodecane thiol caps [34] and nonane thiol passivation [35]. The synthesis of aliphatic nitriles from OLA in the presence of $AgNO_3$ at relatively high temperatures is shown by C-N stretching vibrations, which may be the cause of the absorption [36].

## Crystal features

Figure 3 displays the synthesized OLA-capped AgNPs; XRD patterns. The OLA-capped AgNPs suit the fcc structure of the bulk silver according to the data, with broad peaks at 38°, 44°, 65°, 78° and 82 that correspond to (111), (200), (220), (311) and (222) crystallographic planes, respectively. These peaks are matched with the fcc structure of silver (JCPDS file No. 04-0783) [37]. When the standard Scherrer equation and a geometric factor of 0.89 are used to compute the average crystallite diameters across the (111) reflection, the result for OLA-capped AgNPs was 7.32 ± 2.76 nm. The Scherrer equation (Crystal Size (D) = Kλ/(β Cos θ)) consistently tends to underestimate the true size of the NPs, most likely due to the instrument's contribution to the line width and the structural stress of the AgNPs, as evidenced by the particles' slightly smaller sizes than those determined from TEM images (8.44 ± 1.73 nm).

## Microscopic analysis

TEM was used to confirm the morphological information, shape and particle size of the OLA-capped AgNPs. Figure 4 displays the TEM micrographs (Figure 4a, and histogram (Figure 4b) obtained from Image J software used to determine the size distribution of NPs). The TEM pictures revealed that the synthesized NPs were spherical in shape with non-uniform particle sizes (Figure 4a insert) and with little agglomerations. Both micrographs shows the details of agglomeration and separate NPs and the appearance for a bulk of the particles. This was confirmed by the histogram which showed that the nanoparticles were in the range of 4 - 14 nm, with an

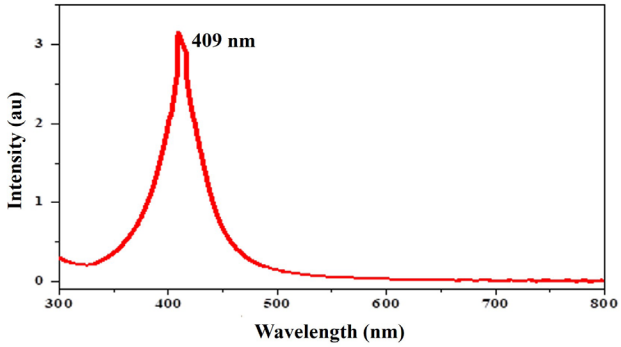



**Figure 1:** UV-Vis spectrum of OLA-capped AgNPs prepared at 180 °C for 1 hour.

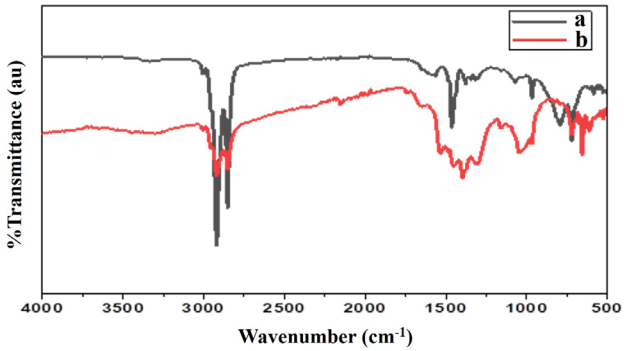



**Figure 2:** FTIR spectra of **(a)** pure OLA and **(b)** OLA-capped AgNPs.

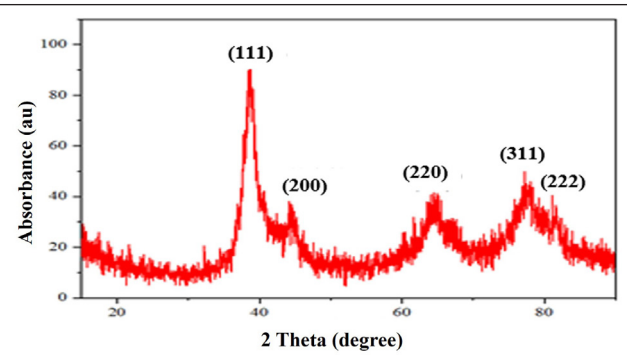



**Figure 3:** XRD pattern of OLA-capped AgNPs prepared at 180 °C for 1 hour and then cooled to 70 °C.

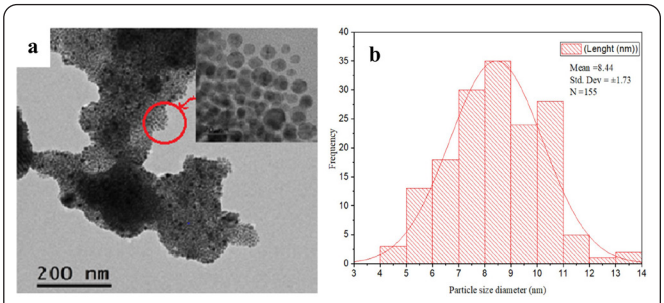



**Figure 4:** TEM images **(a)** of OLA-capped AgNPs and their **(b)** size histogram.

average particle size of 8.44 ± 1.73 nm. A similar study [31], revealed that synthesized nano-silver was sphere form, small size, separation and congruence with an average size was 6.5 ± 0.5 nm. The agglomerations observed could be a result of Ostwald ripening [38]. Chen et al. [36] who performed the same study under different temperature conditions, established that the formation of AgNPs with less or no agglomerations can be achieved by decreasing the temperature. From their findings, they found that the average diameters of the synthesized AgNPs were 9.8 ± 4.7 nm and 14.1 ± 4.4 nm at 140 and 200 °C for more than 8 hours of synthesis time, respectively. Similarly, a relatively high concentration of OLA might cause high particle coverage by an amine, avoiding particle aggregation during the process [37, 38].

EDS was used to quantify the relative quantity of every element present in the prepared OLA-capped AgNPs (Figure 5a and 5b). Figure 5a, represents the area selected for elemental analysis as shown in the SEM-EDS micrograph and the figure 5b shows the EDS spectrum which confimed presence of Ag in the prepared NPs. The EDS analysis confirmed that the particles were pure silver with a considerable amount of carbon and oxygen. These impurities are sought to have come from the capping agent, and adsorbed gaseous molecules [39]. The small amount of oxygen observed could be attributed to the presence of OLA (capping agent), indicating that there was a successful synthesis of AgNPs [40].

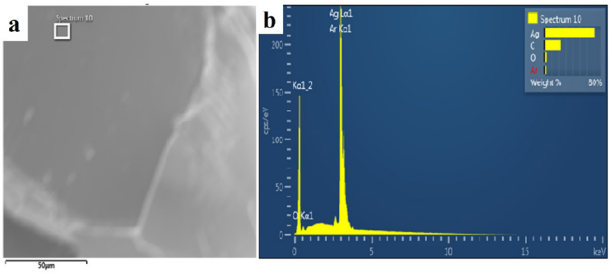



**Figure 5:** Elemental results for OLA-capped AgNPs. **(a)** SEM-EDS micrograph and **(b)** an EDS spectrum.

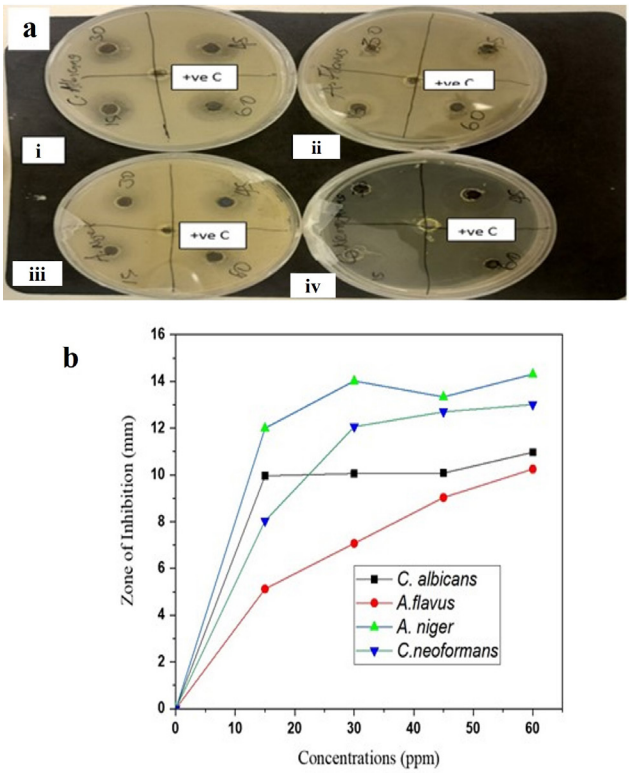



**Figure 6:** Antifungal activity of OLA-capped AgNPs. **(a)** Well-diffusion assay plates against **(i)** *C. albicans*, **(ii)** *A. flavus*, **(iii)** *A. niger*, and **(iv)** *C. neoformans* and **(b)** Graph showing ZOI (mm).

## Anti-fungal activities of OLA-capped AgNPs

Figure 6a and 6b show the analysis of OLA-capped AgNP's inhibitory impact on fungi culture linked with mould growth at various doses. The outcomes showed that all of the test fungi were sensitive to increased OLA-capped AgNPs concentrations (Figure 6b). In comparison to the other three fungal strains, *A. niger* was found to be more susceptible to OLA-capped AgNPs, with ZOI averaging 13.76 mm at a concentration of 30 ppm. The four pathogens under study had their spore germination and mycelium development markedly reduced by the OLA-capped AgNPs. The AgNPs also prevented the signs of fungi growth without leaving any traces on the media. OLA-capped AgNPs' inhibitory effect on the four fungi was found to be proportional to the concentration of OLA-capped AgNPs. The pathogen's inhibition order was found to be; *A. niger* < *C. neoformans* < *C. albicans* < *A. flavus*. A significant difference in the antifungal activity of AgNPs against test fungus (Table 1, $p < 0.05$). The AgNPs showed superior activity (ZOI) against *A. niger* with an average diameter of 14 ± 0.15 mm.

AgNPs are well recognized for increasing the permeability of the cellular membrane of the fungal mycelium and for causing the breakdown of cellular and organelle components [40]. AgNPs affect the pathways involved in glucose metabolism, the tricarboxylic acid cycle, and energy metabolism [41]. This study supported previous studies that determined *A. niger* to be the four moulds' most destructive strain [42]. *C. neoformans* fungi strain followed to be the second most lethal fungi in enhancing mould growth. The four chosen moulds exhibited effective concentration values of AgNPs that were all less than 15 ppm, proving that AgNPs significantly in-

**Table 1:** Antifungal activity (ZOI) of OLA-capped AgNPs.

| Sr. No | Name of organism | Conc. of OLA-capped AgNPs (µg/ml) | | | |
|---|---|---|---|---|---|
| | | 15 | 30 | 45 | 60 |
| 1. | *C. albicans* | 9.90 ± 0.30$^{a}$ | 10.06 ± 0.10$^{a}$ | 10.10 ± 0.10$^{c}$ | 11.06 ± 0.11$^{b}$ |
| 2. | *A. flavus* | 5.12 ± 0.14$^{b}$ | 7.07 ± 011$^{b}$ | 9.03 ± 0.05$^{b}$ | 10.10 ± 0.10$^{c}$ |
| 3. | *A. niger* | 12.00 ± 0.10$^{c}$ | 13.76 ± 0.05$^{c}$ | 13.00 ± 0.15$^{a}$ | 14.00 ± 0.15$^{a}$ |
| 4. | *C. neoformans* | 8.03 ± 0.05$^{d}$ | 12.06 ± 0.06$^{d}$ | 12.08 ± 0.05$^{a}$ | 13.06 ± 0.05$^{d}$ |

**Note:** n = 3; superscript alphabets indicating significant difference ($p < 0.05$).

hibited the growth of mould on grains before harvest. Other research cytological analyses have demonstrated that AgNPs cause significant harm to the cellular components of the fungal cell wall, leading to degradation in cell membrane integrity, spore and mycelial wrinkles, and depression [43, 44]. AgNPs are also known to affect the oxygen consumption of mycelial respiration, block vital respiratory chain enzymes, and cause cell lysis via lipid and enzyme binding [45]. Cell death and withering are the ultimate results of these cumulative effects. These results demonstrate that AgNPs may be used to prevent mould growth, which is a significant issue for agricultural and post-harvest grain crops.

## Conclusion

OLA-capped AgNPs were successfully synthesized and characterized in this study. The confirmation of OLA-capped AgNPs formation was achieved through the observation of a narrow, symmetric extinction peak at approximately 409 nm on the UV-Vis spectra. This distinctive peak is primarily attributed to the primary dipolar excitation of the NPs. Moreover, the spectroscopic analysis revealed the symmetric and asymmetric vibrations peak blue-shift of the -$CH_2$ group, located at 2954 and 2922 $cm^{-1}$, respectively, due to the interactions with the AgNPs. Structural analysis indicated that the OLA-capped AgNPs exhibited a fcc structure similar to the typical silver. The diffraction peaks observed at approximately 38°, 44°,65°, 78° and 82° corresponded to the (111), (200), (220), (311) and (222) lattice planes, respectively. The average particle size of the OLA-capped AgNPs was determined to be 8.44 ± 1.73 nm which demonstrated remarkable antifungal activity against various fungal strains for *A. niger*, *C. neoformans*, *C. albicans*, and *A. flavus*. However, its efficacy was particularly notable against *A. niger* at higher concentrations. The exceptional antifungal properties of the OLA-capped AgNPs suggest their potential use in combating mold growth, which has long been a threat to food security, particularly in the storage of cereals.

## Acknowledgements

The authors are thankful to the Vaal University of Technology, Department of Biotechnology and Chemistry for providing the laboratory facilities, and the facility for the antimicrobial assay. Special thanks due to the Electron Microscopy Unit at the University of Cape Town (UCT) for assisting with the TEM and SEM-EDS analysis.

## Conflict of Interest

All the authors declare that they do not have any competing interests.

### References

1. Ekeh FN, Onah IE, Atama CI, Ivoke N, Eyo JE. 2013. Effectiveness of botanical powders against *Callosobruchus maculatus* (Coleoptera: Bruchidae) in some stored leguminous grains under laboratory conditions. *African J Biotechnol* 12(12): 1384-1391.
2. Agriopoulou S, Stamatelopoulou E, Varzakas T. 2020. Advances in occurrence, importance, and mycotoxin control strategies: prevention and detoxification in foods. *Foods* 9(2): 137. https://doi.org/10.3390/foods9020137
3. Neme K, Mohammed A. 2017. Mycotoxin occurrence in grains and the role of postharvest management as a mitigation strategies. A review. *Food Control* 78: 412-425. https://doi.org/10.1016/j.foodcont.2017.03.012
4. Brock M. 2009. Fungal metabolism in host niches. *Curr Opin Microbiol* 12(4): 371-376. https://doi.org/10.1016/j.mib.2009.05.004
5. Bennett JW, Klich M. 2003. Mycotoxins. *Clin Microbiol Rev* 16(3): 497-516. https://doi.org/10.1128/cmr.16.3.497-516.2003
6. Richard JL. 2007. Some major mycotoxins and their mycotoxicoses—an overview. *Int J Food Microbiol* 119(1-2): 3-10. https://doi.org/10.1016/j.ijfoodmicro.2007.07.019
7. Pitt JI, Hocking AD. 2009. Fungi and Food Spoilage. New York, Springer.
8. Manandhar A, Milindi P, Shah A. 2018. An overview of the post-harvest grain storage practices of smallholder farmers in developing countries. *Agriculture* 8(4): 57. https://doi.org/10.3390/agriculture8040057
9. Kiaya V. 2014. Post-harvest losses and strategies to reduce them. Technical Paper on Postharvest Losses, Action Contre la Faim (ACF).
10. Li DW, Yang CS. 2004. Fungal contamination as a major contributor to sick building syndrome. *Adv Appl Microbiol* 55: 31-112.
11. Kraft S, Buchenauer L, Polte T. 2021. Mold, mycotoxins and a dysregulated immune system: a combination of concern?. *Int J Mol Sci* 22(22): 12269. https://doi.org/10.3390/ijms222212269
12. Sauer DB. 1988. Effects of fungal deterioration on grain: nutritional value, toxicity, germination. *Int J Food Microbiol* 7(3): 267-275. https://doi.org/10.1016/0168-1605(88)90045-1
13. Raza MA, Kanwal Z, Rauf A, Sabri AN, Riaz S, et al. 2016. Size-and shape-dependent antibacterial studies of silver nanoparticles synthesized by wet chemical routes. *Nanomaterials* 6(4): 74. https://doi.org/10.3390/nano6040074
14. Alemayehu S, Abera FA, Ayimut KM, Darnell R, Mahroof R, et al. 2023. Effects of storage duration and structures on sesame seed germination, mold growth, and mycotoxin accumulation. *Toxins* 15(1): 39. https://doi.org/10.3390/toxins15010039
15. Rai M, Yadav A, Gade A. 2009. Silver nanoparticles as a new generation of antimicrobials. *Biotechnol Adv* 27(1): 76-83. https://doi.org/10.1016/j.biotechadv.2008.09.002
16. Roco MC. 2005. International perspective on government nanotechnology funding in 2005. *J Nanopart Res* 7: 707-712. https://doi.org/10.1007/s11051-005-3141-5
17. Sahoo M, Vishwakarma S, Panigrahi C, Kumar J. 2021. Nanotechnology: current applications and future scope in food. *Food Front* 2(1): 3-22. https://doi.org/10.1002/fft2.58
18. Bajpai VK, Kamle M, Shukla S, Mahato DK, Chandra P, et al. 2018. Prospects of using nanotechnology for food preservation, safety, and security. *J Food Drug Anal* 26(4): 1201-1214. https://doi.org/10.1016/j.jfda.2018.06.011
19. Terzi E, Kartal SN, Yılgör N, Rautkari L, Yoshimura T. 2016. Role of various nano-particles in prevention of fungal decay, mold growth and termite attack in wood, and their effect on weathering properties and water repellency. *Int Biodeter Biodegr* 107: 77-87. https://doi.org/10.1016/j.ibiod.2015.11.010
20. Markowska K, Grudniak A, Wolska K. 2013. Silver nanoparticles as an alternative strategy against bacterial biofilms. *Acta Biochim* Pol 60(4): 523-530.
21. Link S, El-Sayed MA. 2000. Shape and size dependence of radiative, non-radiative and photothermal properties of gold nanocrystals. *Int Rev Phys Chem* 19(3): 409-453. https://doi.org/10.1080/01442350050034180
22. Evanoff DD, Chumanov G. 2005. Synthesis and optical properties of silver nanoparticles and arrays. *Chemphyschem* 6(7): 1221-1231. https://doi.org/10.1002/cphc.200500113

23. Chimentao RJ, Kirm I, Medina F, Rodriguez X, Cesteros Y, et al. 2004. Different morphologies of silver nanoparticles as catalysts for the selective oxidation of styrene in the gas phase. *Chem Commun* (7): 846-847. https://doi.org/10.1039/b400762j
24. Gurunathan S, Park JH, Han JW, Kim JH. 2015. Comparative assessment of the apoptotic potential of silver nanoparticles synthesized by *Bacillus tequilensis* and *Calocybe indica* in MDA-MB-231 human breast cancer cells: targeting p53 for anticancer therapy. *Int J Nanomed* 10: 4203-4223. https://doi.org/10.2147/IJN.S83953
25. Li WR, Xie XB, Shi QS, Zeng HY, Ou-Yang YS, et al. 2010. Antibacterial activity and mechanism of silver nanoparticles on *Escherichia coli*. *Appl Microbiol Biotechnol* 85: 1115-1122. https://doi.org/10.1007/s00253-009-2159-5
26. Mukherjee P, Ahmad A, Mandal D, Senapati S, Sainkar SR, et al. 2001. Fungus-mediated synthesis of silver nanoparticles and their immobilization in the mycelial matrix: a novel biological approach to nanoparticle synthesis. *Nano Lett* 1(10): 515-519. https://doi.org/10.1021/nl0155274
27. Żarowska B, Koźlecki T, Piegza M, Jaros-Koźlecka K, Robak M. 2019. New look on antifungal activity of silver nanoparticles (AgNPs). *Pol J Microbiol* 68(4): 515-525. https://doi.org/10.33073/pjm-2019-051
28. More DS, Moloto MJ, Moloto N, Matabola KP. 2015. TOPO-capped silver selenide nanoparticles and their incorporation into polymer nanofibers using electrospinning technique. *Mater Res Bull* 65: 14-22. https://doi.org/10.1016/j.materresbull.2015.01.030
29. Sánchez-López E, Gomes D, Esteruelas G, Bonilla L, Lopez-Machado AL, et al. 2020. Metal-based nanoparticles as antimicrobial agents: an overview. *Nanomaterials* 10(2): 292. https://doi.org/10.3390/nano10020292
30. Desai R, Mankad V, Gupta SK, Jha PK. 2012. Size distribution of silver nanoparticles: UV-visible spectroscopic assessment. *Nanosci Nanotechnol Lett* 4(1): 30-34. https://doi.org/10.1166/nnl.2012.1278
31. Truong MKT, Dang DMT, Tran MQT, Dang CM. 2021. Synthesis of silver nanoparticles capped by Oleylamine, application for conductive film production. *IOSR J Eng* 11(06): 1-6.
32. Jain J, Arora S, Rajwade JM, Omray P, Khandelwal S, et al. 2009. Silver nanoparticles in therapeutics: development of an antimicrobial gel formulation for topical use. *Mol Pharm* 6(5): 1388-1401. https://doi.org/10.1021/mp900056g
33. Ulman A. 1991. Ultrathin Organic Films: From Langmuir-Blodgett to Self-Assembly. Academic Press, Boston.
34. Korgel BA, Fullam S, Connolly S, Fitzmaurice D. 1998. Assembly and self-organization of silver nanocrystal superlattices: ordered "soft spheres". *J Phys Chem B* 102(43): 8379-8388. https://doi.org/10.1021/jp981598o
35. He S, Yao J, Xie S, Gao H, Pang S. 2001. Superlattices of silver nanoparticles passivated by mercaptan. *J Phys D Appl Phys* 34(24): 3425. https://doi.org/10.1088/0022-3727/34/24/301
36. Chen M, Feng YG, Wang X, Li TC, Zhang JY, et al. 2007. Silver nanoparticles capped by oleylamine: formation, growth, and self-organization. *Langmuir* 23(10): 5296-5304. https://doi.org/10.1021/la700553d
37. Lanje AS, Sharma SJ, Pode RB. 2010. Synthesis of silver nanoparticles: a safer alternative to conventional antimicrobial and antibacterial agents. *J Chem Pharm Res* 2(3): 478-483.
38. Sun Y, Yin Y, Mayers BT, Herricks T, Xia Y. 2002. Uniform silver nanowires synthesis by reducing $AgNO_3$ with ethylene glycol in the presence of seeds and poly (vinyl pyrrolidone). *Chem Mater* 14(11): 4736-4745. https://doi.org/10.1021/cm020587b
39. Lin XZ, Teng X, Yang H. 2003. Direct synthesis of narrowly dispersed silver nanoparticles using a single-source precursor. *Langmuir* 19(24): 10081-10085. https://doi.org/10.1021/la035185c
40. Zhang XF, Liu ZG, Shen W, Gurunathan S. 2016. Silver nanoparticles: synthesis, characterization, properties, applications, and therapeutic approaches. *Int J Mol Sci* 17(9): 1534. https://doi.org/10.3390/ijms17091534
41. Pietrzak K, Glińska S, Gapińska M, Ruman T, Nowak A, et al. 2016. Silver nanoparticles: a mechanism of action on moulds. *Metallomics* 8(12): 1294-1302. https://doi.org/10.1039/c6mt00161k
42. Babele PK, Singh AK, Srivastava A. 2019. Bio-inspired silver nanoparticles impose metabolic and epigenetic toxicity to Saccharomyces cerevisiae. *Front Pharmacol* 10: 1016. https://doi.org/10.3389/fphar.2019.01016
43. Li L, Pan H, Deng L, Qian G, Wang Z, et al. 2022. The antifungal activity and mechanism of silver nanoparticles against four pathogens causing kiwifruit post-harvest rot. *Front Microbiol* 13: 988633. https://doi.org/10.3389/fmicb.2022.988633
44. More PR, Pandit S, Filippis AD, Franci G, Mijakovic I, et al. 2023. Silver nanoparticles: bactericidal and mechanistic approach against drug resistant pathogens. *Microorganisms* 11(2): 369. https://doi.org/10.3390/microorganisms11020369
45. Nie P, Zhao Y, Xu H. 2023. Synthesis, applications, toxicity and toxicity mechanisms of silver nanoparticles: a review. *Ecotoxicol Environ Safety* 253: 114636. https://doi.org/10.1016/j.ecoenv.2023.114636